Pergamon

Available online at www.sciencedirect.com
SCIENCE DIRECT®

Cement and Concrete Research 34 (2004) 1297–1305

CEMENT AND CONCRETE RESEARCH

Thaumasite–ettringite solid solutions in degraded mortars

S.M. Torres[a,b], C.A. Kirk[c], C.J. Lynsdale[a], R.N. Swamy[b], J.H. Sharp[c]

[a]*Department of Civil and Structural Engineering, Centre for Cement and Concrete, University of Sheffield, Mappin Street, Sheffield S1 3JD, UK*
[b]*Department of Mechanical Engineering, Centre for Cement and Concrete, University of Sheffield, Mappin Street, Sheffield S1 3JD, UK*
[c]*Department of Engineering Materials, Centre for Cement and Concrete, University of Sheffield, Mappin Street, Sheffield S1 3JD, UK*

Received 29 May 2003; accepted 16 September 2003

Abstract

The thaumasite form of sulfate attack (TSA) has been observed in mortar prisms made from Portland–limestone cements after laboratory storage in 1.8% magnesium sulfate solution at 5 °C for 5 years. The prisms all showed evident signs of degradation, which increased with increasing limestone content. X-ray powder diffraction indicated that a solid solution was formed in all the prisms, which was based on the crystal structure of thaumasite, but extended towards the chemical composition of ettringite. The prism made from the cement with the highest level (35%) of limestone replacement gave the greatest amount of the thaumasite solid solution and had a composition close to the thaumasite end member, whereas those cements with lower (15%, 5% and 0%) levels of replacement gave reduced amounts of the solid solution and had greater lattice parameters. The solid solutions that have been observed are compared with those reported by Barnett et al. for synthetic thaumasite samples grown from sucrose solution.

Keywords: Crystal structure; X-ray diffraction; Sulfate attack; Ettringite; Thaumasite

1. Introduction

It has become apparent in recent years that the thaumasite form of sulfate attack (TSA) can initiate serious degradation in mortars and concretes made from ordinary (ASTM Type I) and sulfate-resisting (ASTM Type V) Portland cements [1–3]. Crammond [3] has reported that TSA has been found in more than 80 field structures and buildings in the UK, while instances of TSA in other countries, particularly where cool, damp conditions prevail, are becoming common [2,4–6]. Thaumasite forms very readily in the laboratory when pastes, mortars or concretes made from Portland cement are stored at low temperatures (< 15 °C) in the presence of a source of carbonate ions, such as limestone filler or limestone or dolomite aggregate, and an external supply of sulfate ions from a solution containing sodium, magnesium or calcium sulfate.

Thaumasite, $Ca_3[Si(OH)_6 \cdot 12H_2](SO_4)(CO_3)$, is structurally related to ettringite, $Ca_6[Al(OH)_6 \cdot 12H_2O]_2$ $(SO_4)_3 \cdot 2H_2O$, a common product from the hydration of tricalcium aluminate in the presence of sulfate ions in Portland cement [7]. The crystal structure of thaumasite is most unusual in that the silicon atoms are octahedrally coordinated by $(OH)^-$ ions instead of the tetrahedral coordination found in almost all the mineral silicates. It is not surprising therefore that thaumasite and ettringite form a solid solution in which Si atoms are replaced by Al in these octahedral sites. The anion substitutions are, however, more complex as the charge has to be reduced to compensate for the lower oxidation state of Al(III) compared with that of Si(IV). In ettringite, therefore, a quarter of the available anion sites are filled by water molecules; while in thaumasite, an ordered arrangement of equal numbers of sulfate and carbonate ions occupy the anion sites. Overall, the replacements are best summarised by comparing one formula unit of ettringite with two formula units of thaumasite:

$$\underset{\text{ettringite}}{Ca_6[Al(OH)_6 \cdot 12H_2O]_2(SO_4)_3(H_2O)_2} \leftrightarrows \underset{\text{thaumasite}}{Ca_6[Si(OH)_6 \cdot 12H_2O]_2(SO_4)_2(CO_3)_2}$$

This solid solution and related solid solutions have been thoroughly researched recently in an important series of

---

* Corresponding author. Tel.: +44-114-222-5504; fax: +44-114-222-5943.

E-mail address: j.h.sharp@sheffield.ac.uk (J.H. Sharp).

0008-8846/$ – see front matter © 2003 Elsevier Ltd. All rights reserved.
doi:10.1016/j.cemconres.2003.09.016

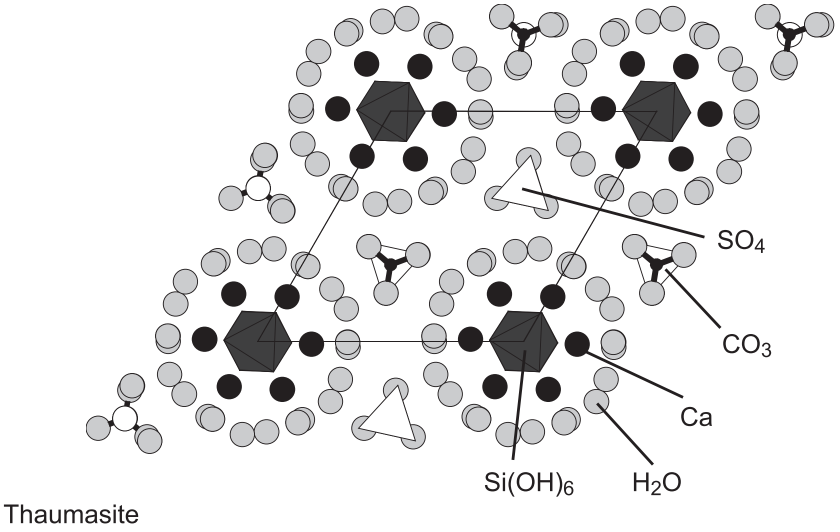

Fig. 1. Crystal structure of thaumasite–projection on *a*–*b* plane.

papers by Barnett et al. [8–12]. The unit cell of ettringite is trigonal, based on space group P31c, with $a = 11.234$ Å and $c = 21.501$ Å [13–15]; whereas the unit cell of thaumasite is hexagonal, based on space group $P6_3$, with $a = 11.055$ Å and $c = 10.410$ Å [12,14,16–18]. The *a*–*b* projection of thaumasite (based on the atomic coordinates given by Jacobsen et al. [18]) is shown in Fig. 1 and that for ettringite is closely similar but slightly larger. At each corner of the unit cell of ettringite, there is a cylindrical column of composition $Ca_3[Al(OH)_6 \cdot 12H_2O]_{3+}$ that runs parallel to the *c*-axis as shown in Fig. 2, which is based on the atomic coordinates given by Moore and Taylor [13]. The sulfate anions and the remaining water molecules lie in channels running parallel to these columns. Thaumasite is comprised of similar columns and

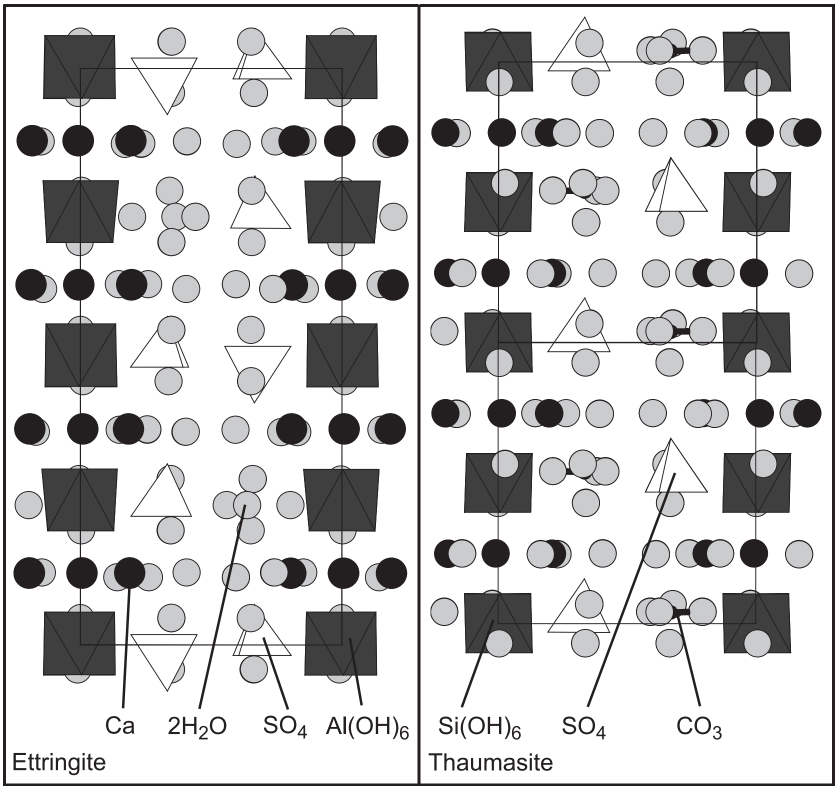

Fig. 2. Crystal structure of thaumasite and ettringite–$(11\bar{2}0)$ projection with *c*-dimension vertical.

channels to those found in ettringite, except that Si replaces Al in the columns, while $2(SO_4)^{2-}$ and $2(CO_3)^{2-}$ replace 3 $(SO_4)^{2-}$ and $2H_2O$ in the channels (Fig. 2). The smaller silicon atoms are stabilised in octahedral coordination by charge transfer through the hydroxyl groups to the calcium ions (in eightfold coordination) and onward to the water molecules that are hydrogen bonded to the sulfate and carbonate anions [15,19].

The anion arrangement in thaumasite allows an ordered arrangement of alternating sulfate and carbonate ions to be formed in the *c*-direction, as shown in Fig. 2, hence resulting in the different space group and the halved *c*-dimension of the unit cell compared with that of ettringite. Barnett et al. [8,12] have stated that these differences suggest that a discontinuity may exist in the solid solution. They used pure chemicals to synthesise a series of samples with compositions between the end members. Barnett et al. [8] used X-ray diffraction and full pattern fitting to characterise these phases and to determine their lattice parameters. Two distinct structural types were observed. The thaumasite-type formed a cluster with *a*-dimensions between 11.05 and 11.11 Å, while the ettringite-type had *a*-dimensions between 11.17 and 11.23 Å. There was a gap in the *a*-dimension between 11.11 and 11.17 Å into which no phase fell, which was attributed to a probable discontinuity in the solid solution [8]. The corresponding values in the *c*-dimension were not specifically quoted.

Subsequently, Barnett et al. [10] investigated three series of solid solutions using Rietveld refinement of the XRD data. The solid solutions fell into two groups separated by a gap in the *c*-dimension between 20.95 and 21.25 Å based on ettringite (or 10.475 and 10.625 Å based on thaumasite). Phases with *c*-dimensions less than 10.475 Å were assumed to have the thaumasite structure and the maximum value for *a* seems to have been about 11.09 Å.

The question arises whether such solid solutions are formed in the degradation products produced by the TSA of mortar and concrete or whether the thaumasite end member is formed. Recently, Torres et al. [20] have reported on the condition of Portland–limestone cement mortar prisms after storage in air and in 1.8% magnesium sulfate solution at 5 °C for 5 years. The prisms stored in magnesium sulfate all showed clear signs of deterioration that increased in intensity with increasing limestone content. As the level of limestone replacement decreased from 35% to 0%, the XRD peaks attributed to thaumasite shifted to lower angles, suggesting that a solid solution of the type reported by Barnett et al. [8,10,11] had formed. The XRD data in our previous study [20] were obtained using a Siemens-D500 diffractometer at scanning speeds of $2°2\theta$/min and $0.5°2\theta$/min. The aim of the present investigation was to reinvestigate these specimens using a high resolution Stoe STADI P diffractometer and software suite WinXPow to determine accurate lattice parameters.

2. Experimental

The samples used in this investigation were obtained from test specimens made more than 5 years ago and reported previously [21,22]. The mortar prisms, 40 × 40 × 160 mm, were made using a cement to aggregate ratio of 1:2.5 and a water to binder (cement plus limestone powder) ratio of 0.5. The limestone powder additions replaced the Portland cement, mass for mass, at three levels of 5%, 15% and 35%. The Portland cement was of typical normal composition, with a C_3A content of 8.5% based on a conventional Bogue calculation. The limestone was Carboniferous with a calcium carbonate content greater than 98% and a mean particle size of 0.21 μm. Full chemical analyses of both these materials have already been published [21,23]. The sand used in the mortar specimens was Normensand, a German standard quartz sand, conforming to BS EN 196-1. The prisms were cured in water for 27 days after demolding and then exposed to air at 5 °C or completely submerged in 1.8% $MgSO_4$ solution at 5 °C. The solution was changed every 3 months for a period of 4 years, after which the solution was allowed to evaporate gradually, still at 5 °C. The specimens were more than 5 years old at the time of the characterisation studies reported here.

Powder XRD data were collected on a STOE STADI P diffractometer in transmission mode with a small linear position sensitive detector, Ge monochromator and either $CoK\alpha_1$ or $CuK\alpha_1$ radiation. Data were collected over the range $8 \leq 2\theta \leq 70°$ with a detector step width of $0.1°2\theta$ and a count time of 50 s per step. The anatase form of TiO_2 (20%) was added to the samples, prior to the data collection, as an internal standard. The data were then analysed using the program INDEX, part of the software suite WinXPow. This method was preferred to Rietveld refinement because it is a more direct way to obtain the information required (i.e., lattice parameters only). The systems under investigation are multiphase and to carry out Rietveld refinement, structural models of all the phases involved are required, but it is difficult to obtain starting models for some of them because their compositions are uncertain.

First, the data were corrected for zero point error using the internal standard. Peak positions were then determined using a peak search algorithm. The peaks associated with TiO_2, SiO_2, $CaCO_3$ and $CaSO_4 \cdot 2H_2O$ were eliminated, and the remaining peaks that were associated with the ettringite- or thaumasite-type phases were used as input data of the refinement of the lattice parameters. The refinement procedure is a least squares method, which requires as input data a starting model of the unit cell (lattice parameters, crystal system and space group) to calculate the theoretical peak positions and the observed peak positions of the phase under investigation. The program then assigns an *hkl* to an observed peak if it is within a preset 2θ range of a theoretical peak (calculated from the starting model). The differences in 2θ

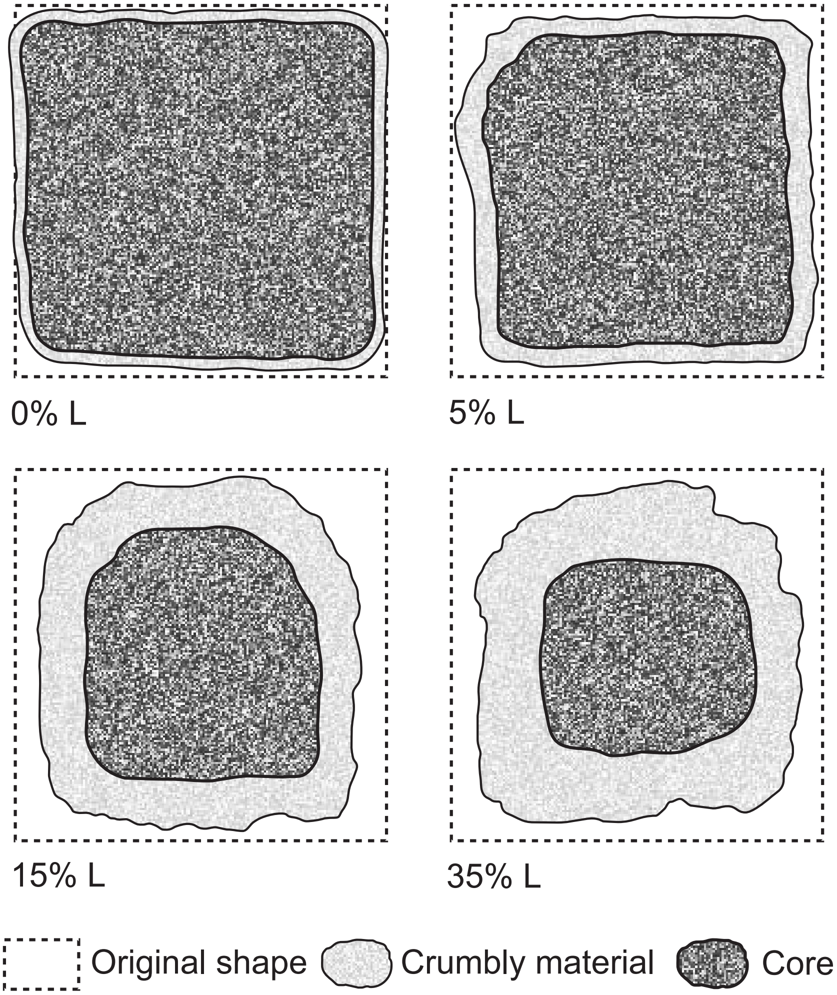

Fig. 3. Schematic of the cross-sectional view of mortar prisms stored in 1.8% $MgSO_4$ solution at 5 °C for 5 years (L = limestone).

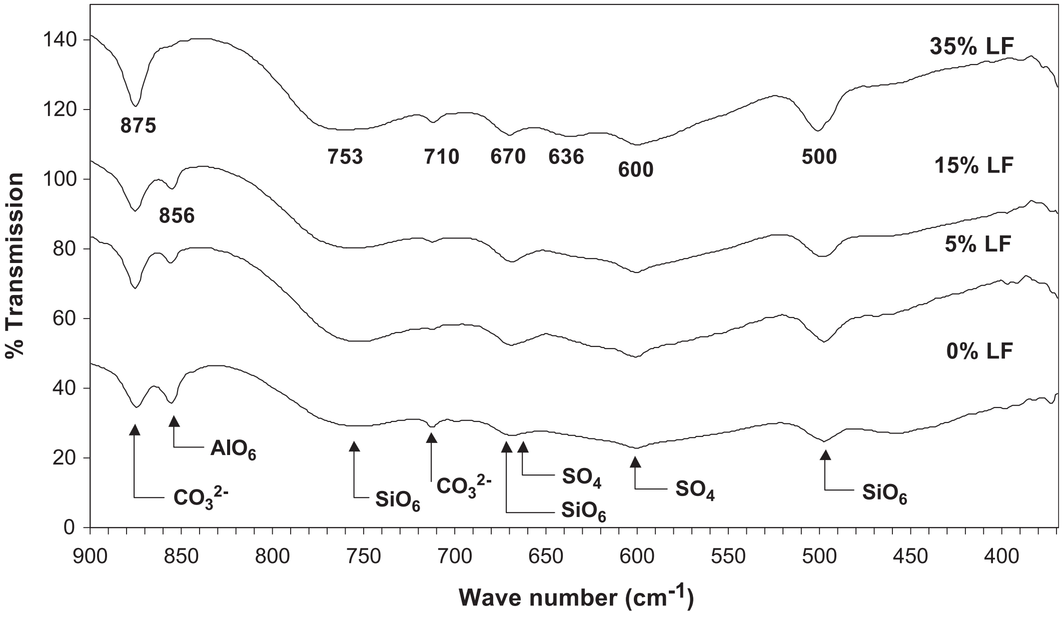

Fig. 4. Infrared spectra of degraded parts of Portland–limestone cement mortars stored in 1.8% $MgSO_4$ solution at 5 °C for 5 years.

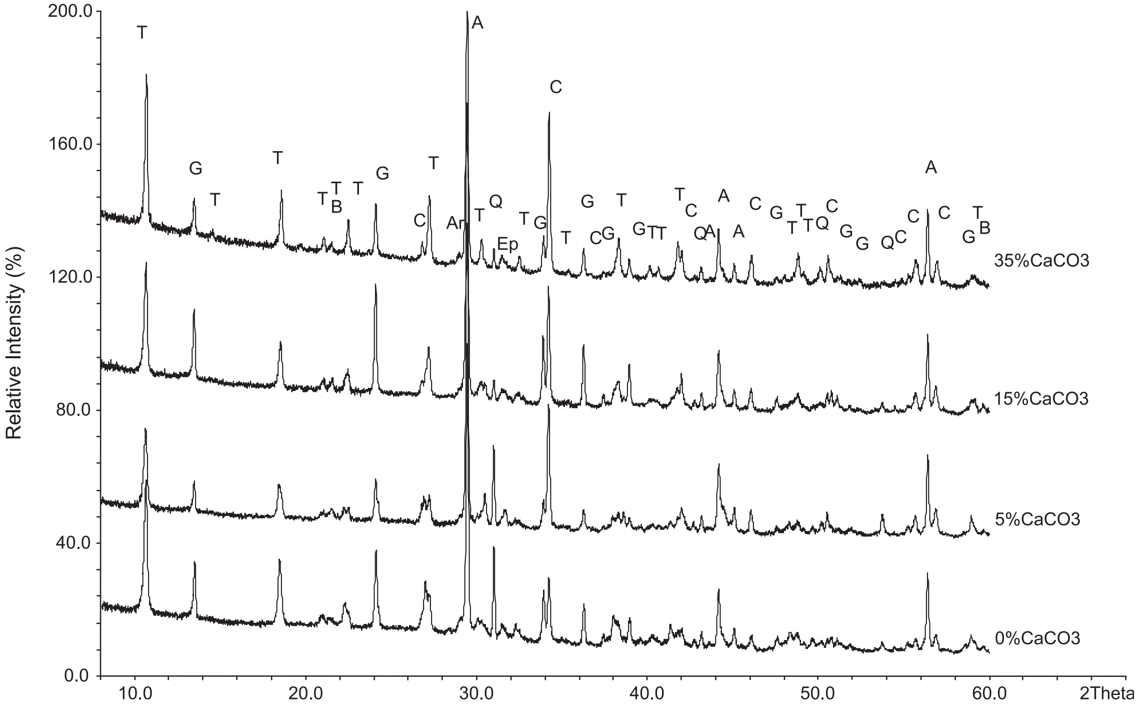

Fig. 5. X-ray diffraction pattern (5–60°2θ) of degraded parts of Portland–limestone cement mortars stored in 1.8% $MgSO_4$ solution at 5 °C for 5 years obtained using coradiation. A = anatase (internal standard), Ar = aragonite, B = brucite, C = calcite, Ep = epsomite, G = gypsum, Q = quartz, T = thaumasite.

between the observed and theoretical peaks are then minimised via a least squares procedure, which alters the input lattice parameters. In this way, the refined lattice parameters for the phase under investigation are obtained. The error in the determination of the lattice parameters is estimated to be ± 0.005 Å.

IR spectra were obtained from KBr discs using a Perkin-Elmer FT-IR 2000 spectrometer. The 12-mm discs were

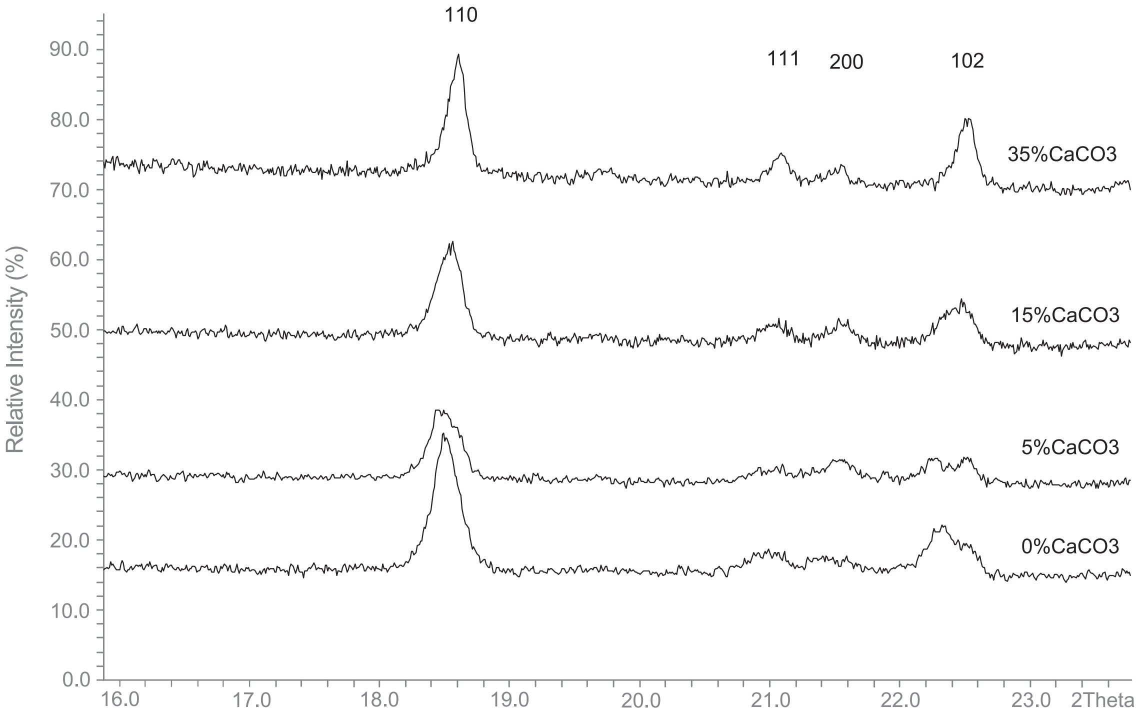

Fig. 6. X-ray diffraction pattern (17–23°2θ) of degraded parts of Portland–limestone cement mortars stored in 1.8% MgSO4 solution at 5 °C for 5 years obtained using coradiation.

Table 1
Limestone replacement levels of the cements and lattice parameters of the thaumasite-based solid solutions

%$CaCO_3$	a (Å)	c (Å)	2c (Å)
0	11.140	10.550	21.100
5	11.130	10.430	20.860
15	11.090	10.470	20.940
15 *	11.090	10.465	20.930
35	11.060	10.425	20.850
Thaumasite ettringite	11.055	10.410	20.820
	11.234		21.501†

* Separate sample (see text).

† *c* Parameter of ettringite.

prepared using 2 mg of sample with 198 mg of KBr, ground manually in an agate mortar and pestle until a fine homogeneous powder was obtained that could be pressed.

3. Results

3.1. Visual inspection

The appearance of the prisms after storage in 1.8% $MgSO_4$ solution for 5 years is shown in Fig. 3, which represents a schematic cross-sectional view based on the fuller account reported previously [20]. All the prisms had degraded, but the intensity of the corrosive attack was greater as the level of limestone replacement increased. The degradation commenced at the corners and edges of the prism (see 0% limestone sample), leading to spalling initially at the corners (5% limestone sample) and subsequently to total disintegration of the surface material (15% and 35% limestone samples).

3.2. Infrared spectroscopy

The key region of the IR spectra, from 375 to 900 cm^{-1}, of the four samples is shown in Fig. 4. The peak at 500 cm^{-1} is assigned to the presence of octahedral silicon atoms coordinated to oxygen atoms, whereas that at 860 cm^{-1} is assigned to Al-O-H [24]. The former peak is strongest in the sample containing 35% limestone filler, whereas the latter peak is almost absent in this sample, but prominent in the other three spectra, especially for the sample with no limestone filler. The full IR spectra of these samples have been reported elsewhere [20]. Because octahedral silicon is so rare in mineral silicates, the presence of the peak at 500 cm^{-1} is indicative that either thaumasite or a solid solution based on either thaumasite or ettringite and incorporating octahedral silicon must be present in the sample.

3.3. X-ray diffraction

The XRD patterns of the four samples, obtained using coradiation, are shown in Fig. 5. The peak positions for thaumasite were determined by comparison with those in the literature [17,18]. The 2θ values differ from those shown elsewhere [8–12,20,22,23] because the wave length of coradiation (1.78897 Å) is different from that of Cu (1.54056 Å). The 2θ region 17°–23° (equivalent to *d*-spacings from 3.06 to 2.29 Å) is shown in Fig. 6, and (*hkl*) values are attributed to various peaks based on the unit cell of thaumasite. It is clear from the data that a phase related to both thaumasite and ettringite is present and that the peak positions shift with increasing limestone content towards the thaumasite end member, indicating the presence of a thaumasite-type solid solution. The Miller indices indicated in Fig. 6 relate to the unit cell of

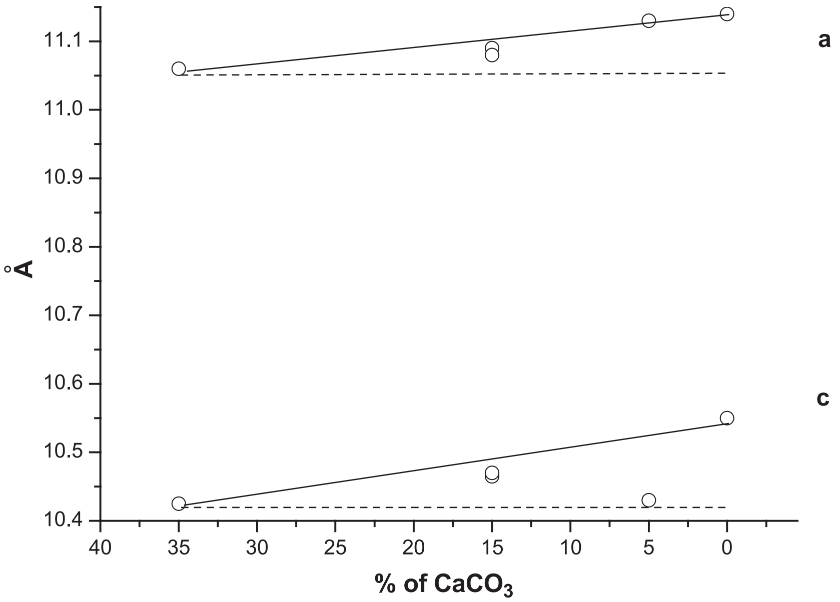

Fig. 7. Plot of lattice parameters of the thaumasite-based solid solution against level of limestone replacement in the Portland–limestone cements.

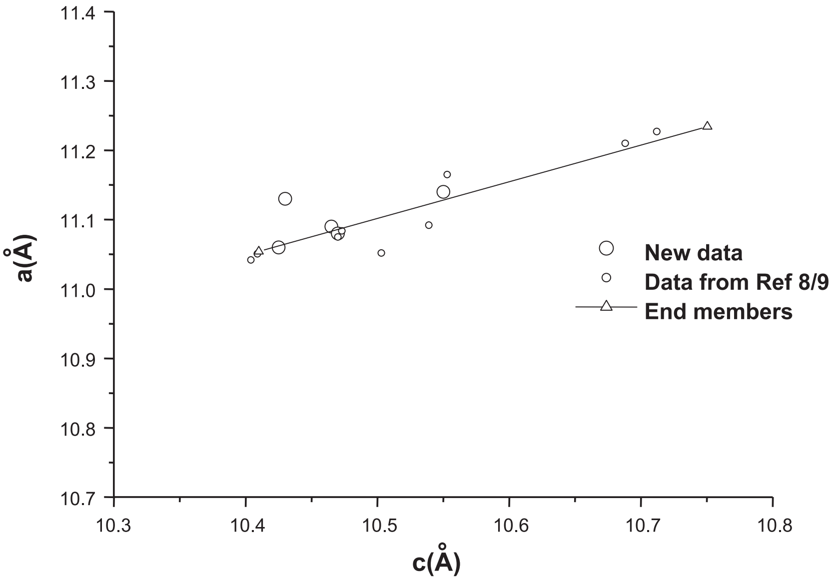

Fig. 8. Plot of *a* versus *c* for thaumasite-based solid solutions from this work (○), from Barnett et al. [8,9] (○) and the end members (△).

thaumasite. The peaks associated with this phase were indexed in space group P63 for each sample and the resulting lattice parameters are given in Table 1 to the nearest 0.005 Å; note that the *c* parameters have also been doubled for comparison with the lattice parameter of ettringite. The two values for samples containing 15% limestone filler are from separate prisms and agree remarkably well.

The lattice parameters are plotted against the limestone content in the cement in Fig. 7. It can be noted that (a) there is (fortuitously) an almost linear decrease in both *a* and *c* with increasing limestone content, (b) the magnitude of this change is greater for *c* than for *a* and (c) the lattice parameters for the sample with 35% limestone are very close to those for the thaumasite end member. The *c*-value for the 5% $CaCO_3$ sample is below the line but is still greater than that of thaumasite itself.

A plot of *a* against *c* is shown in Fig. 8 with our data superimposed on data tabulated by Barnett et al. [10,11] for several thaumasite-related solid solutions and two ettringite-related solid solutions. The data from the present study occupy the region at the thaumasite end of the solid solution range and generally fit well with the data of Barnett et al. The point for the 5% limestone cement sample is displaced from the line connecting the lattice parameters of thaumasite and ettringite. The point for the sample without any limestone filler is discussed below.

4. Discussion

The mortar prisms used in this investigation were originally made by Hartshorn et al. [22] and it was shown that thaumasite was readily formed within a few months in the mortars with 15% and 35% of the OPC replaced by limestone. Additional information concerning the condition of the prisms after 1 year has been provided elsewhere [21,22].

Subsequently, these samples were reexamined after 5 years by Torres et al. [20] when the extent of the degradation caused by storage in magnesium sulfate solution was much greater, even in the prism made with only 5% limestone replacement. It was concluded from a thorough characterisation of these samples using XRD and FTIR that the damage to the samples containing limestone filler, including that with only 5% replacement of Portland cement, was due to the TSA. It was also noted that the XRD data seemed to indicate that less thaumasite was present as the level of limestone replacement decreased and that the composition of the phase changed, suggesting that it involved a solid solution of the type investigated by Barnett et al. [8,10–12].

The results of the XRD investigation presented here confirm this conclusion. The importance of this observation is that these results have been obtained on laboratory-cured mortar prisms made from commercial samples of Portland cement and limestone, whereas the earliest observations of Barnett et al. [8,10] were based on samples synthesised using reagent-grade chemicals and grown from sucrose solutions. The similarity of the data obtained on cement matrix-derived phases to those in synthetic thaumasite solid solutions provides important validation of the laboratory-based approach to predicting behaviour in the field.

Recently, Barnett et al. [11] have reported the formation of thaumasite-based solid solutions in mixes containing carbonate-bearing aggregates at higher water/ solid ratios and ettringite-based solid solutions in mixtures made from a composite cement in which 70% of the

Portland cement had been replaced by blast furnace slag. It seems reasonable to conclude, based on the observations presented in this paper and those of Barnett et al. [11], that whenever thaumasite has been identified in mortars and concrete, it has been in the form of a solid solution of the type reported here. Indeed, it is unlikely that the stoichiometric thaumasite end member will be precipitated from a cement paste solution, which is always likely to contain some aluminate ions.

As discussed in Section 1, Barnett et al. [8] have suggested that the thaumasite-based solid solution extends from an *a*-dimension of 11.054 Å to around 11.11 Å and a *c*-dimension of 10.41 Å to around 10.475 Å [10]. The three samples with the greatest amounts of thaumasite solid solution reported here (two with 15% limestone replacement and one with 35% limestone replacement) fit comfortably within these limits. The relatively high value for *a* in the 5% $CaCO_3$ sample may indicate the formation of a sulfate-rich thaumasite solid solution in which the SO_4:CO_3 ratio is greater than 1 [25]; alternatively, it may be that the *c* parameter is low (see Fig. 7). The sample based on zero limestone replacement should strictly not have formed any thaumasite solid solution, unless it gained carbonate ions from atmospheric CO_2 or through contamination from the solution in which the other samples were also immersed. There was evidence in this sample (see Fig. 6) for the formation of two solid solutions, but the peaks were weaker than those observed at the three levels of limestone replacement. One possibility is the formation of an ettringite-type solid solution as well as a thaumasite-type solid solution, as observed by Barnett et al. [8,10,12]; however, the presence of the former could not be definitely confirmed because the intensities of the peaks at higher angles were too weak. Another possibility is that the sample contained a somewhat different type of solid solution similar to that reported by Barnett et al. [10] in the mortar from the Waterloo and City Underground Station in London, which had lattice parameters of $a = 11.165$ Å and $c = 10.553$ Å, close to those reported in Table 1 for the 0% limestone sample. The Waterloo and City sample was reported to contain no aluminium and to have had a high sulfate content compared with that of thaumasite. Our sample too could have a high sulfate content relative to its carbonate content because it had no limestone incorporated in it and was immersed in a strong sulfate solution. There was, however, some uncertainty in the indexing scheme of the high angle peaks. The intensities of these peaks are weak due to the presence of two or more solid solutions in this sample, and hence there is more uncertainty in the lattice parameters of the solid solution present in this sample than those in the other samples.

Overall, the results presented here are in good accord with those of Barnett et al. [8,10–12] but might indicate that the thaumasite-type solid solution extends to a slightly higher value of *a* than 11.11 Å. The maximum *c* value for the thaumasite-type solid solution of about 10.475 Å [12] is confirmed for the samples reported here, except for the one with zero limestone replacement, which may be unreliable for the reasons discussed above. Values greater than 10.475 Å for the *c* parameter of thaumasite solid solutions have been reported recently by Barnett et al. [10,11] and may reflect greater complexity in the solid solution than mere replacement of Si by Al, such as carbonate-rich or sulfate-rich compositions.

5. Conclusions

- Mortar prisms made from Portland–limestone cement and even from Portland cement, stored in 1.8% $MgSO_4$ solution at 5 °C, have suffered serious deterioration after 5 years due to the TSA.
- The extent of the attack increased with increasing replacement of Portland cement by fine limestone.
- The thaumasite formed varied in its lattice parameters because it was part of a solid solution extending partway towards the composition of ettringite.
- The extent of $(CO_3)^{2-}$ for $(SO_4)^{2-}$ replacement increased with increasing limestone replacement. Whereas the sample based on 35% replacement had lattice parameters very close to those of the thaumasite end member, the sample with no replacement formed less thaumasite solid solution and had lattice parameters higher than the limits proposed by Barnett et al. [8,10,12].
- Because thaumasite in cementitious products must be formed via a through solution mechanism from a pore solution that inevitably contains some aluminate ions, it is likely to form as a solid solution rather than as the stoichiometric end member.

Acknowledgements

We are grateful to CAPES-Brazil for providing a scholarship to SMT. We wish to thank Mike Chapman and Wendy Dutton for their help in the preparation of the manuscript.

References

[1] The UK Government Thaumasite Expert Group, The thaumasite form of sulfate attack: Risks, diagnosis, remedial works and guidance on new construction, Report of the Thaumasite Expert Group, Department of the Environment, Transport and the Regions: London, January, 1999.

[2] N.J. Crammond, The occurrence of thaumasite in modern construction—A review, Cem. Concr. Compos. 24 (2002) 393–402.

[3] N.J. Crammond, The thaumasite form of sulfate attack in the UK, Proceedings of the 1st International Conference on Thaumasite in Cementitious Materials, held at the Building Research Establishment, Watford, UK, June, Cem. Concr. Compos. (in press).

[4] M. Romer, L. Holzer, M. Pfiffner, Swiss tunnel structures: concrete damage by formation of thaumasite, Proceedings of the 1st Interna-

tional Conference on Thaumasite in Cementitious Materials, held at the Building Research Establishment, Watford, UK, June, Cem. Concr. Compos. (in press).

[5] P. Hagelia, R.G Sibbick, N.J. Crammond, C.K. Larsen, Thaumasite and secondary calcite in some Norwegian concretes, Proceedings of the 1st International Conference on Thaumasite in Cementitious Materials, held at the Building Research Establishment, Watford, UK, June, Cem. Concr. Compos. (in press).

[6] J.S. Suput, A. Mladenovic, L. Cernilogar, V. Olensk, Deterioration of mortar caused by the formation of thaumasite on the limestone cladding of Slovenian railway tunnels, Proceedings of the 1st International Conference on Thaumasite in Cementitious Materials, held at the Building Research Establishment, Watford, UK, June, Cem. Concr. Compos. (in press).

[7] H.F.W. Taylor, Cement Chemistry, 2nd ed., Thomas Telford Publishing, London, 1997.

[8] S.J. Barnett, C.D. Adam, A.R.W. Jackson, Solid solutions between ettringite, $Ca_6Al_2(SO_4)_3(OH)_{12}\cdot 26H_2O$, and thaumasite, $Ca_3SiSO_4CO_3(OH)_6\cdot 12H_2O$, J. Mater. Sci. 35 (2000) 4109–4114.

[9] S.J. Barnett, C.D. Adam, A.R.W. Jackson, An XRPD profile fitting investigation of the solid solution between ettringite, $Ca_6Al_2(SO_4)_3(OH)_{12}\cdot 26H_2O$, and carbonate ettringite, $Ca_6Al_2(CO_3)_3(OH)_{12}\cdot 26H_2O$, Cem. Concr. Res. 31 (2001) 13–17.

[10] S.J. Barnett, D.E. Macphee, N.J. Crammond, Solid solutions between thaumasite and ettringite and their role in sulfate attack, Concr. Sci. Eng. 3 (2001) 209–215.

[11] S.J. Barnett, M.A. Halliwell, N.J. Crammond, C.D. Adam, A.R.W. Jackson, Study of thaumasite and ettringite phases formed in sulfate/blast furnace slag slurries using XRD full pattern fitting, Cem. Concr. Compos. 24 (2002) 339–346.

[12] S.J. Barnett, D.E. MacPhee, E.E. Lachowski, N.J. Crammond, XRD, EDX and IR analysis of solid solutions between thaumasite and ettringite, Cem. Concr. Res. 32 (2002) 719–730.

[13] A.E. Moore, H.F.W. Taylor, Crystal structure of ettringite, Acta Crystallogr., B 26 (1970) 386–393.

[14] L.J. Struble, Synthesis and characterisation of ettringite and related phases, 8th International Congress on Chemical Cement, Rio de Janeiro vol. VI, (1987) 582–588.

[15] H. Pollmann, H.-J. Kuzel, R. Wenda, Compounds with ettringite structure, Neues Jahrb. Mineral. Abh. 160 (1989) 133–158.

[16] R.A. Edge, H.F.W. Taylor, Crystal structure of thaumasite, $[Ca_3Si(OH)_6\cdot 12H_2O](SO_4)(CO_3)$, Acta Crystallogr., B 27 (1971) 594–601.

[17] S.J. Barnett, C.D. Adam, A.R.W. Jackson, P.D. Hywel-Evans, Identification and characterisation of thaumasite by XRPD techniques, Cem. Concr. Compos. 21 (1999) 123–128.

[18] S.D. Jacobsen, J. Warwick, J.R. Smyth, R.J. Swope, Single crystal X-ray diffraction study of the Si(IV)-OH and Si(VI)-OH bonds in pectolite and thaumasite, respectively, at room pressure and temperatures from 25 to − 130 °C, Abstract EDS Trans., Amer. Geophys. Union 77 (1996) 144–145.

[19] R.A. Edge, H.F.W. Taylor, Crystal structure of thaumasite, a mineral containing $Si(OH)_6$ groups, Nature 224 (1969) 363–364.

[20] S.M. Torres, J.H. Sharp, R.N. Swamy, C.J. Lynsdale, A. Huntely, Long term durability of Portland–limestone cement mortars exposed to magnesium sulfate attack, Proceedings of the 1st International Conference on Thaumasite in Cementitious Materials, held at the Building Research Establishment, Watford, UK, June, Cem. Concr. Compos. (in press).

[21] S.A. Hartshorn, R.N. Swamy, J.H. Sharp, Engineering properties and structural implications of Portland–limestone cement mortar exposed to magnesium sulfate attack, Adv. Cem. Res. 13 (2001) 31–46.

[22] S.A. Hartshorn, J.H. Sharp, R.N. Swamy, The thaumasite form of sulfate attack in Portland–limestone cement mortars stored in magnesium sulfate solutions, Cem. Concr. Compos. 24 (2002) 351–359.

[23] S.A. Hartshorn, J.H. Sharp, R.N. Swamy, Thaumasite formation in Portland–limestone cement pastes, Cem. Concr. Res. 29 (1999) 1331–1340.

[24] J. Bensted, S.P. Varma, Studies of thaumasite: Part II, Silic. Ind. 39 (1974) 11–19.

[25] J.H. Sharp, C.A. Kirk, unpublished results.